2013

Controls on recent Alaskan lake changes identified from water isotopes and remote sensing

Lesleigh Anderson
USGS, land@usgs.gov

Jennifer Rover
Earth Resource Observation and Science, U.S. Geological Survey

Nikki Gaulager
Yukon Flats National Wildlife Refuge

Jean Birks
Alberta Innovates Technology Futures

GEOPHYSICAL RESEARCH LETTERS, VOL. 40, 3413–3418, doi:10.1002/grl.50672, 2013

Controls on recent Alaskan lake changes identified from water isotopes and remote sensing

Lesleigh Anderson,[1] Jean Birks,[2] Jennifer Rover,[3] and Nikki Guldager[4]

Received 13 May 2013; revised 13 June 2013; accepted 16 June 2013; published 12 July 2013.

[1] High-latitude lakes are important for terrestrial carbon dynamics and waterfowl habitat driving a need to better understand controls on lake area changes. To identify the existence and cause of recent lake area changes in the Yukon Flats, a region of discontinuous permafrost in north central Alaska, we evaluate remotely sensed imagery with lake water isotope compositions and hydroclimatic parameters. Isotope compositions indicate that mixtures of precipitation, river water, and groundwater source ~95% of the studied lakes. The remaining minority are more dominantly sourced by snowmelt and/or permafrost thaw. Isotope-based water balance estimates indicate 58% of lakes lose more than half of inflow by evaporation. For 26% of the lakes studied, evaporative losses exceeded supply. Surface area trend analysis indicates that most lakes were near their maximum extent in the early 1980s during a relatively cool and wet period. Subsequent reductions can be explained by moisture deficits and greater evaporation.
Citation: Anderson, L., J. Birks, J. Rover, and N. Guldager (2013), Controls on recent Alaskan lake changes identified from water isotopes and remote sensing, *Geophys. Res. Lett.*, *40*, 3413–3418, doi:10.1002/grl.50672.

1. Introduction

[2] The likelihood of future warming trends in Alaska has motivated efforts to observe and evaluate recent hydrologic change [*Hinzman et al.*, 2005; *Walvoord et al.*, 2012]. Theory and climate models suggest greater Arctic precipitation with a warming atmosphere that is supported to some extent by Eurasian river discharge since the 1940s [*Peterson et al.*, 2002]. However, a significant degree of interannual discharge variability is also linked with regional atmospheric dynamics such as those characterized by the Northern Annual Mode and Pacific Decadal Oscillation and/or El Niño–Southern Oscillation in the North Pacific sector [*Brabets and Walvoord*, 2009; *Cassano and Cassano*, 2010]. Other surface water trends, such as lake volume and area, are currently ambiguous, with a diversity of variation observed in continuous and discontinuous permafrost regions [*Riordan et al.*, 2006; *Smith et al.*, 2005]. Lake surface observations are available in Alaska from early aerial photographic surveys beginning in the late 1950s and by satellite data since the late 1970s.

[3] Lake surface areas, and corresponding volume, reflect the balance between rates of surface inflow, groundwater discharge, and precipitation falling directly onto a lake, with rates of water loss from surface outflow, groundwater recharge, and evaporation/evapotranspiration from the lake surface and surrounding wetlands. At high latitudes, permafrost distribution may be the most important factor in determining lake density in addition to surface flow [*Williams*, 1970]. In areas of continuous permafrost, subpermafrost groundwater is often isolated from the surface, and there are unique mechanisms for thermokarst lake dynamics such as lateral expansion and breaching [*Jones et al.*, 2011; *Labrecque et al.*, 2009; *Plug et al.*, 2008]. Groundwater-surface water interactions in the interior regions of Alaska are more commonly found in areas of discontinuous permafrost [e.g., *Minsley et al.*, 2012; *Walvoord et al.*, 2012].

[4] Here the focus is on a region of discontinuous permafrost in northeast Alaska known as the Yukon Flats (YF) that encompasses the ~118,340 km^2 low-lying area surrounding the confluence of the Yukon and Porcupine rivers (Figure 1). YF lakes occupy depressions formed by fluvial, eolian, and thermokarst processes, have a wide diversity of sizes and shapes, and remain frozen for 7 to 8 months of each year. In general, shallower basins with more gradual slopes undergo larger changes in surface extent for incremental changes in volume than deeper counterparts with steep sides. This is likely one reason why YF lakes exhibit complex spatial patterns of change for different temporal scales [*Roach et al.*, 2011; *Rover et al.*, 2012].

[5] Lake water isotope ratios provide a useful measure for characterizing lake hydrology. Isotopes of oxygen and hydrogen in lake water are sensitive to hydrologic processes, and in particular, the preferential loss of light isotopes by evaporation. Here we also derive estimates of the ratio of water lost by evaporation to that gained by inflow (E/I) by using an isotope-based water balance model. The isotope labels are also used to identify the dominant sources for lakes such as mixtures of rainfall and snowfall, groundwater, rivers, or thawed permafrost [e.g., *Wolfe et al.*, 2007]. These parameters are then used in conjunction with climatic data and remotely sensed imagery to identify the patterns and causes of recent lake area changes.

2. Study Area and Methods

[6] The YF is a region of extreme seasonal temperature difference and low precipitation (<250 mm/yr) [*Shulski and Wendler*, 2007]. Potential evapotranspiration (PET) estimates,

Additional supporting information may be found in the online version of this article.

[1]Geosciences and Environmental Change, U.S. Geological Survey, Denver, Colorado, USA.
[2]Alberta Innovates Technology Futures, Calgary, Alberta, Canada.
[3]Earth Resource Observation and Science, U.S. Geological Survey, Sioux Falls, South Dakota, USA.
[4]Yukon Flats National Wildlife Refuge, Fairbanks, Alaska, USA.

Corresponding author: L. Anderson, Geosciences and Environmental Change, U.S. Geological Survey, Denver, CO 80225, USA. (land@usgs.gov)

0094-8276/13/10.1002/grl.50672

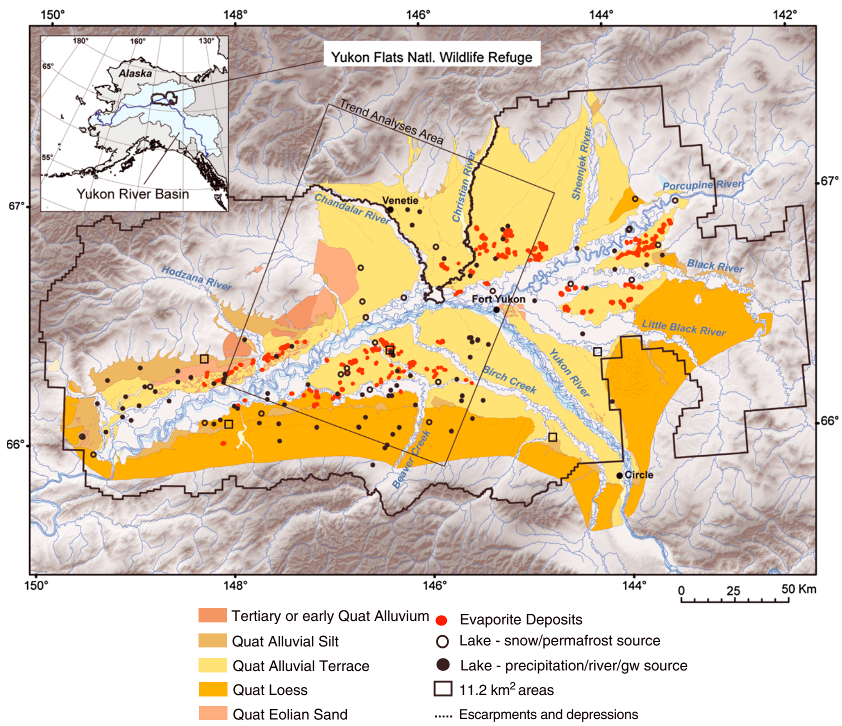

Figure 1. The surficial geology of the Yukon Flats National Wildlife Refuge from *Williams* [1962] is shown on a digital elevation model (30 m) with lake locations for this study, the location of evaporite deposits from *Clautice and Mowatt* [1981], and the 11.2 km^2 areas delineated by *Heglund and Jones* [2003] within which 59 lakes were sampled in 2011 (individual lake locations not shown). The rectangular box encloses the area of the surface area trend analysis. Open circle symbols indicate lakes sourced by snow and/or permafrost.

following *Hogg* [1997], indicate annual moisture deficits near 15 cm/yr. Lakes are generally fresh to moderately brackish (<1600 μS) and predominantly eutrophic or hypereutrophic [*Hawkins*, 1995; *Heglund and Jones*, 2003]. Evaporite salt films occur on lake margins and dry lakebeds (Figure 1) and consist of trona, calcite, dolomite, gypsum, and halite [*Clautice and Mowatt*, 1981]. Vegetation is a mosaic of grassy meadows, muskeg, marsh, and forests of spruce and birch that are highly prone to fire [*Drury and Grissom*, 2008].

[7] Lake water isotope samples from 83 lakes were acquired in July, August, or September between 2007 and 2010 by fixed wing aircraft (Figure 1; supporting information text). An additional set of smaller lakes ($n = 33$) was sampled by helicopter in September 2009. In July 2011, 59 lakes were sampled on foot within five distinct 11.2 km^2 areas that were previously defined and investigated for baseline limnology [*Heglund and Jones*, 2003]. River water data used here are from *Schuster et al.* [2010] collected during the months of June through October between 2006 and 2008 from the Yukon River at Circle and Fort Yukon, the Porcupine River above Fort Yukon, and the Chandalar River above Venetie. Water for isotope analysis was collected in 30 mL Nalgene high density polyethylene or glass bottles that were filled to minimize headspace, sealed to prevent evaporation and analyzed within 2 months of collection. Water samples were prepared for oxygen and hydrogen isotope ratio analyses by automated constant temperature equilibration with CO_2, and automated D/H preparation by chromium reduction, coupled to an isotope ratio mass spectrometer and are reported in δ-notation relative to Vienna standard mean ocean water (VSMOW). Analytical precision is ± 0.08‰ and ± 0.9‰ for oxygen and hydrogen, respectively.

[8] Lake evaporation-to-inflow ratios (E/I) were calculated using the isotope mass balance method developed by *Gibson and Edwards* [2002] which assumes a well-mixed lake undergoing evaporation while maintaining a long-term constant volume and lake water residence time (see supporting information text for additional information). The method requires isotope values for inflow, lake water, and evaporated vapor and utilizes the assumption that the oxygen isotope ratios of outflow are equivalent to lake water values. The isotopic composition of evaporated vapor is difficult to measure but has been shown to be dependent on temperature, boundary layer state, relative humidity, and the isotopic composition of atmospheric moisture.

[9] Of the 175 lakes sampled for water isotopes, 54 of them were analyzed for surface area changes and trends following the approach described in *Rover et al*. [2012] with additional analysis for 2010 and 2011. There was classification of 22 Landsat Multispectral Scanner, Thematic Mapper, and Enhanced Thematic Mapper Plus scenes during the ice-free season since 1979. Following a decision tree approach, water and nonwater classes were identified, and a total of 16,371 water bodies in the study area had detectable water at more than one date and were not connected to perennial streams and rivers. The water images were converted to vector polygons for calculating area at each image date [*Rover et al*., 2011]. When clouds, cloud shadows, or snow obstructed underlying water bodies, the observation was assigned a "no data" value. Trend analyses are based on a linear regression method with date and water area as the predictor and response, respectively, and the slope representing change in water area per time. A two-tailed *t* test of the slope was used

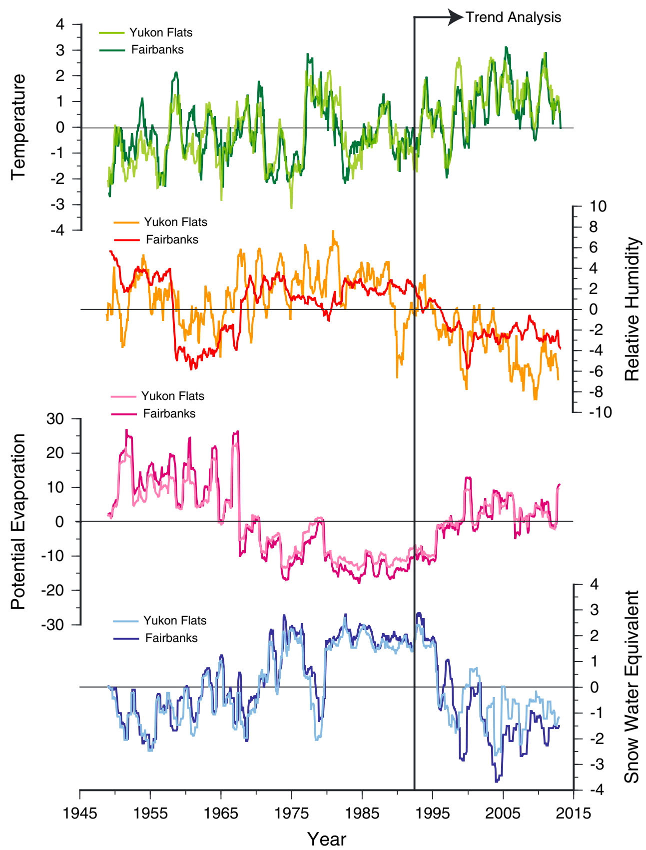

Figure 2. Hydroclimatic parameters for an average of YF grid cells since 1948 to 2012 derived from NCEP-NCAR reanalysis shown with the data for the Fairbanks grid cell. Temperature (°C), relative humidity (%), potential evaporation rate (W/m^2), and snow water equivalent (kg/m^2) are shown as anomalies from the 1948–2012 mean.

to evaluate results for *p*-values ≥ 0.01. Notably, some lakes with insignificant linear regressions are found to have highly variable surface area extents.

[10] Meteorological data since 1948 was obtained from the National Centers for Environmental Prediction-National Center for Atmospheric Research (NCEP-NCAR) reanalysis [*Kalnay et al.*, 1996] for an average of grid cells that encompass the YF area (Figure 2). They are compared with the grid cell for Fairbanks, the location of the nearest first-order climate station 230 km to the south. The records show that following an arid period during the 1950s, higher relative humidity, greater snowfall, and lower potential evaporation characterize the period between ~1970 and 1995, a change that has been attributed to natural variability of the position and strength of the Aleutian Low [*Hartmann and Wendler*, 2005]. From the mid-1990s to the present day, temperatures have been relatively high, humidity levels low, snowfall low, and potential evaporation high.

3. Results

[11] The oxygen and hydrogen isotope ratios of lakes range from −20‰ to −5‰ and −85‰ to −160‰, respectively (Figure 3 and Tables S1 and S2). Lakes are generally enriched in heavy isotopes with respect to meteoric waters as represented by the Global Meteoric Water Line (GMWL), which is an indication of kinetic fractionation effects during evaporation. Lakes are also enriched relative to the average value for Yukon River waters (−21‰ for oxygen and −167‰ for hydrogen), which as an integration of all regional waters is typically similar to the average isotopic values of precipitation and approximates the values for groundwater. The majority of lakes plot on an evaporation line with a slope of 5 that intersects the GMWL near the average Yukon River value. This intersection indicates that the source water for most lakes is a mixture of precipitation and groundwater in addition to river water for lakes with surface connections or within floodplains.

[12] For a small group of lakes (26 of 175), plotting a line through their position to the average river water value was found to produce unreasonably low slopes ($m \approx 3$) that are inconsistent with regionally established slopes of 4.5 to 5.5 [*Gibson et al.*, 2002] and suggest alternative source waters. Therefore, we regressed an evaporation line with a slope of 5 from each of these lakes (see supporting information text

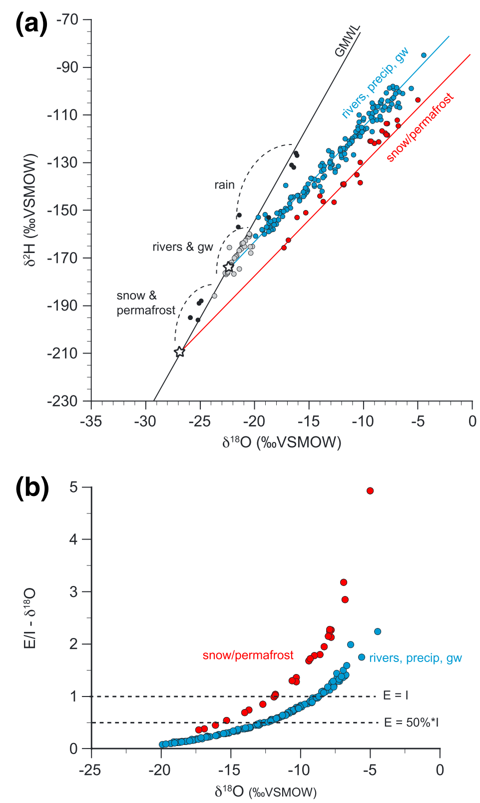

Figure 3. Oxygen and hydrogen isotopes and calculated evaporation-to-inflow (E/I) ratios of water in the Yukon Flats: (a) Lake isotope ratios shown with the Global Meteoric Water Line (GMWL), and estimated monthly precipitation values (black) [*Bowen and Revenaugh*, 2003], and Yukon, Porcupine, and Chandalar River values (gray) [*Schuster et al.*, 2010]. Dashed arcs indicate the approximate ranges of isotope values for rain, snow, rivers, groundwater, and permafrost. Blue circles indicate lakes sourced by combinations of precipitation, rivers, and groundwater, and red circles indicate those sourced by snowmelt and/or permafrost thaw. Stars indicate approximate source values for each group. (b) Colors similar to Figure 2a show the populations of lakes with E/I > 0.5 and 1, above which evaporation losses are greater than 50% and 100% of inflow, respectively.

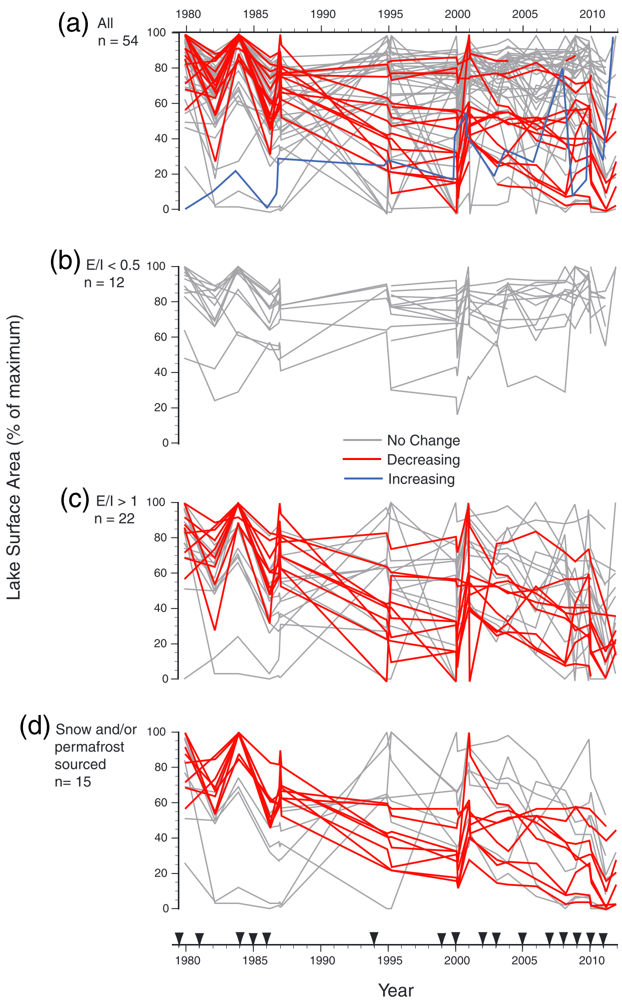

Figure 4. Change in lake extent as a % of maximum from 1979 to 2011 for (a) all 54 lakes sampled within the trend analysis area, (b) lakes with E/I < 0.5 (n = 12), (c) lakes with E/I > 1 (n = 22), and (d) lakes sourced by snowmelt and/or thawed permafrost (n = 15). Image acquisition years are indicated as black triangles on the horizontal time scale. Gray lines indicate lakes with no surface area trends, red lines indicate lakes with decreasing trends, and a blue line for the one lake with an increasing trend.

for additional discussion) and found that they intersect the GMWL near −27‰ for oxygen and −200‰ for hydrogen, values that are within the range of observed values for snowmelt and permafrost thaw [*Lachniet et al.*, 2012; *Meyer et al.*, 2010]. This suggests that this group of lakes is sourced by snowmelt and permafrost thaw, most likely as talik growth. Reliance on snowmelt and/or permafrost thaw for annual recharge would be more likely for basins that are isolated from deep, subpermafrost groundwater and surface flow. E/I estimates range from 0.08 to 4.93 for the data set (Figure 3b) and are affected by the isotope composition of source waters.

[13] The oxygen and hydrogen isotope compositions, and E/I ratios of the 54 lakes analyzed for area changes span a similar range as the larger data set. Fifteen are dominantly sourced by snowmelt and/or thawed permafrost. Time series of surface areas indicate that more lakes were nearer their maximum extent and generally varied coherently between 1980 and 1990 (Figure 4a). Subsequently, particularly after the mid-1990s, more lakes decreased or varied more significantly. Lakes that underwent less evaporation (E/I < 0.5) tended to have varied less in area, with no overall tendency to increase or decrease (Figure 4b). In contrast, lakes that underwent more evaporation (E/I > 1) tended to have varied more and often in opposing directions; some lakes completely disappeared while others reached their maximum areas (Figure 4c). The lakes identified as sourced by snowmelt/permafrost tended to have varied more, occupied smaller depressions, and had higher evaporation losses (Figure S1). A decreasing trend is evident for several of them since the early 2000s (Figure 4d). A summary of area trends for the different ranges of E/I is shown in Table 1.

4. Discussion

[14] The isotope results indicate that an integration of rainfall, snowfall, river inflow and/or flooding, and groundwater, is the water source for most YF lakes. Therefore, we propose that lake water budgets and area/volume variations are dominantly controlled by hydroclimate, including amounts of precipitation gain, evaporation loss, water table heights, and groundwater flow rates. Comparison with the climate data support this notion as the lakes that have diminished have done so concurrently with lower snowfall, relative humidity, and higher temperatures since ~1995 (Figures 2 and 4). Less moisture on multiannual to decadal time scales likely leads to lower water table heights and reduced subsurface and surface inflows. This may explain the greater diversity of responses as lake levels lower because corresponding surface area depends on basin shape, and there is a great diversity of basin shapes. Regional water table heights and groundwater flow rates are not known within the YF, but airborne electromagnetic imaging has revealed surface-groundwater connections [*Minsley et al.*, 2012]. Taliks beneath larger water bodies were found to extend below the maximum depth of permafrost, allowing surface-groundwater connections, whereas smaller, shallower lakes with smaller taliks were typically isolated.

[15] The lake water isotope results also indicate that snowmelt and/or permafrost thaw is a dominant water source for smaller, shallower lakes that have dramatically varied in extent, by either total water loss and subsequent gain, or steady diminishment (Figure 4d). These lakes were generally more evaporated (Figure 3b), indicating limited groundwater interaction that is consistent with a location within permafrost or other aquatards. Subsurface drainage of lakes due to thawing permafrost and talik growth has been proposed as a mechanism for lake area reductions in other regions of Alaska [*Yoshikawa and Hinzman*, 2003]. Here, however, the isotope data suggest that lakes that could be within permafrost undergo significant water losses by evaporation. The

Table 1. Lake Area Linear Regression Analyses ($p < 0.01$) for E/I and Source

	Number	Increasing	No Change	Decreasing
E/I < 0.5	12	0	12	0
0.5 < E/I < 1.0	20	0	15	5
E/I >1.0	22	1	12	9
Precip/river/groundwater	39	1	32	6
Snowmelt/permafrost thaw	15	0	7	8
Total	54	1	39	14

geophysical evidence within the YF suggests complex groundwater flow paths and surface water connections such that subsurface conduits developed by permafrost thaw seem as likely to provide groundwater to a lake basin as drain it.

[16] There is no known evidence for thermokarst drainage in the YF similar to that which occurs in continuous permafrost regions [*Jones et al*., 2011]. However, snowmelt can recharge small, isolated basins by flowing over a frozen, and/or through a thawed, active layer (i.e., suprapermafrost flow), but isotope labeling cannot distinguish snowmelt versus thawed permafrost in this region because their ranges of values overlap. Nevertheless, the isotope data are consistent with the idea of recent reductions in snowfall as a mechanism for net water loss in some YF lakes [*Jepsen et al*., 2012].

[17] The E/I estimates of the entire 175 lake data set indicate that ~58% of lakes have evaporation losses that exceed 50% of inflow, which is strong evidence for the importance of evaporation in regional YF lake water budgets. We acknowledge that E/I estimates are derived from water isotope data that integrates hydrologic processes for an unknown, and possibly varying, time period that precedes the sample date. This, and the fact that the calculations utilize mean climate state variables from reanalysis data, all introduce sources of uncertainty that we take into consideration for our conclusions here. However, the assumption of constant volume and residence time relative to the time incorporated by the isotope data appears to be generally valid for isolated lakes that were highly evaporated. Indeed, our observations indicate minimal isotopic variation within seasons or from year to year (Figures S2 and S3).

[18] These results lead to the conclusion that the majority of recent lake area reductions in the Yukon Flats can be explained as a response to a multidecadal climate trend toward greater moisture deficit since the mid-1990s. This was characterized by increasing temperatures but also by reduced snowfall and summer humidity. Such a hydroclimatic mechanism may also be a dominant driver for other interior regions of Alaska and high-latitude regions. We cannot definitively rule out individual lake reductions related to permafrost thaw, but the isotope survey indicates that this mechanism is a potential influence on a relatively small number of YF lakes (26 of 175). An important implication of these results is that future surface water variations are likely to remain a function of decadal-scale regional atmosphere circulation variations that control storm tracks and the moisture balance in the Alaskan interior even as warmer global temperatures become more likely. Decadal-scale climate variation in Alaska is documented for the past 1000 years and the Holocene from paleohydroclimatic data [*Anderson et al*., 2007; *Barber et al*., 2004]. Such atmospheric dynamics are currently beyond the simulation ability of climate models, but the data in this study highlight their primary importance.

[19] The data also reveal remarkable hydrologic diversity at the watershed scale. It is notable that the range of isotope and E/I values within very small $<10\,km^2$ areas is nearly equivalent to the range of values observed for the entire $\sim 118{,}340\,km^2$ area (Figure S5). Similar hydrologic diversity at smaller spatial scales has been observed in other lake-rich landscapes [*Euliss et al*., 2004; *Turner et al*., 2010] and poses significant challenges for accurately "scaling-up" sparsely sampled areas to draw conclusions that span beyond local to regional controls. These findings indicate that attempts to project future high-latitude lake change will benefit from considering the effects of decadal-scale hydroclimatic variations. Furthermore, isotope ratios of lake water strengthen the basis upon which the vulnerability of individual water bodies and lake regions can be assessed.

[20] **Acknowledgments.** The USGS Climate and Land Use Change R&D Program and the USFWS Yukon Flats National Wildlife Refuge supported this research. We thank Tyler Lewis for providing 2011 water samples. Chris Eastoe, University of Arizona Environmental Isotope Laboratory, provided isotope data; Paco VanSistine provided GIS support. We thank John Gibson for early insights into the data and Ted Hogg for CMI and P-PET estimates. We appreciate manuscript reviews by Tyler Lewis, Brent Wolfe, and anonymous reviewers that helped to improve the manuscript. Any use of trade, firm, or product names is for descriptive purposes only and does not imply endorsement by the U.S. Government.

[21] The Editor thanks Brent Wolfe and an anonymous reviewer for their assistance in evaluating this paper.

References

Anderson, L., et al. (2007), Late Holocene moisture balance variability in the southwest Yukon Territory, Canada, *Quat. Sci. Rev.*, *26*, 130–141.

Barber, V. A., et al. (2004), Reconstruction of summer temperatures in interior Alaska from tree-ring proxies: Evidence for changing synoptic climate regimes, *Clim. Change*, *63*, 91–120.

Bowen, G. J., and J. Revenaugh (2003), Interpolating the isotopic composition of modern meteoric precipitation, *Water Resour. Res.*, *39*(10), 1299, doi:10.1029/2003WR002086.

Brabets, T. P., and M. A. Walvoord (2009), Trends in streamflow in the Yukon River Basin from 1944 to 2005 and the influence of the Pacific Decadal Oscillation, *J. Hydrol.*, *371*, 108–119, doi:10.1016/j.jydrol.2009.03.018.

Cassano, E. N., and J. J. Cassano (2010), Synoptic forcing of precipitation in the Mackenzie and Yukon River basins, *Int. J. Climatol.*, *30*, 658–674, doi:10.1002/joc.1926.

Clautice, K. H., and T. C. Mowatt (1981), Trona occurrences within the Yukon Flats Basin, Alaska, *U.S. Bureau of Mines Open File Rep.*, *69-81*, 34 pp., Washington, D.C.

Drury, S. A., and P. J. Grissom (2008), Fire history and fire management implications in the Yukon Flats National Wildlife Refuge, interior Alaska, *For. Ecol. Manage.*, *256*, 304–312.

Euliss, N. H., et al. (2004), The wetland continuum: A conceptual framework for interpreting biological studies, *Wetlands*, *24*, 448–458.

Gibson, J. J., and T. W. D. Edwards (2002), Regional water balance trends and evaporation-transpiration partitioning from a stable isotope survey of lakes in northern Canada, *Global Biogeochem. Cycles*, *16*(2), 1026, doi:10.1029/2001GB001839.

Gibson, J. J., E. E. Prepas, and P. McEachern (2002), Quantitative comparison of lake throughflow, residency, and catchment runoff using stable isotopes: Modeling and results from a regional survey of boreal lakes, *J. Hydrol.*, *262*, 128–144.

Hartmann, B., and G. Wendler (2005), The significance of the 1976 Pacific climate shift in the climatology of Alaska, *J. Clim.*, *18*, 4824–4839.

Hawkins, D. B. (1995), Geochemistry of saline lakes of the northeastern Yukon Flats, east central Alaska, *Alaska Div. Geol. Geophys. Surv. Prof. Rep.*, *117*, pp. 11–18, Anchorage, AK.

Heglund, P. J., and J. R. Jones (2003), Limnology of shallow lakes in the Yukon Flats National Wildlife Refuge, interior Alaska, *Lake Reserv. Manage.*, *19*(2), 133–140.

Hinzman, L. D., et al. (2005), Evidence and implications of recent climate change in Northern Alaska and other Arctic regions, *Clim. Change*, *72*, 251–298.

Hogg, E. H. (1997), Temporal scaling of moisture and the forest-grassland boundary in western Canada, *Agric. For. Meteorol.*, *84*, 115–122.

Jepsen, S. M., et al. (2012), Sensitivity analysis of lake mass balance in discontinuous permafrost: The example of disappearing Twelvemile Lake, Yukon Flats, Alaska (USA), *Hydrogeol. J.*, *21*, 185–200, doi:10.1007/s10040-10012-10896-10045.

Jones, B. M., G. Grosse, C. D. Arp, M. C. Jones, K. M. Walter Anthony, and V. E. Romanovsky (2011), Modern thermokarst lake dynamics in the continuous permafrost zone, northern Seward Peninsula, Alaska, *J. Geophys. Res.*, *116*, G00M03, doi:10.1029/2011JG001666.

Kalnay, E., et al. (1996), The NCEP/NCAR 40-yr reanalysis project, *Bull. Am. Meteorol. Soc.*, *77*, 437–470.

Labrecque, S., et al. (2009), Contemporary (1951–2001) evolution of lakes in Old Crow Basin, northern Yukon Canada: Remote sensing, numerical modeling, and stable isotope analysis, *Arctic*, *62*, 225–238.

Lachniet, M. S., et al. (2012), Revised ^{14}C dating of ice wedge growth in interior Alaska to MIS2 reveals cold paleoclimate and carbon recycling in ancient permafrost terrain, *Quat. Res.*, *78*, 217–225.

Meyer, H., L. Schirrmeister, K. Yoshikawa, T. Opel, S. Wetterich, H.-W. Hubberten, and J. Brown (2010), Permafrost evidence for severe winter cooling during the Younger Dryas in North America, *Geophys. Res. Lett.*, *37*, L03501, doi:10.1029/2009GL041013.
Minsley, B. J., et al. (2012), Airborne electromagnetic imaging of discontinuous permafrost, *Geophys. Res. Lett.*, *39*, L02503, doi:10.1029/2011GL050079.
Peterson, B. J., et al. (2002), Increasing river discharge to the Arctic Ocean, *Science*, *298*, 2171–2173.
Plug, L. J., C. Walls, and B. M. Scott (2008), Tundra lake changes from 1978 to 2001 on the Tuktoyaktuk Peninsula, western Canadian Arctic, *Geophys. Res. Lett.*, *35*, L03502, doi:10.1029/2007GL032303.
Riordan, B., D. Verbyla, and A. D. McGuire (2006), Shrinking ponds in subarctic Alaska based on 1950–2002 remotely sensed images, *J. Geophys. Res.*, *111*, G04002, doi:10.1029/2005JG000150.
Roach, J., B. Griffith, D. Verbyla, and J. Jones (2011), Mechanisms influencing changes in lake area in Alaskan boreal forest, *Global Change Biol.*, *17*(8), 2567–2583, doi:10.1111/j.1365-2486.2011.02446.x.
Rover, J., C. K. Wright, N. H. Euliss Jr., D. M. Mushet, and B. K. Wylie (2011), Classifying the hydrologic function of Prairie Potholes with remote sensing and GIS, *Wetlands*, *31*, 319–327, doi:10.1007/s13157-011-0146-y.
Rover, J., L. Ji, B. K. Wylie, and L. L. Tieszen (2012), Establishing water body areal extent trends in interior Alaska from multi-temporal Landsat data, *Remote Sens. Lett.*, *3*(7), 595–604, doi:10.1080/01431161.2011.643507.
Schuster, P. F., et al. (2010), Water quality in the Yukon River Basin, Alaska, water years 2006–2008, *U.S. Geol. Surv. Open File Rep., 2010-1241*.
Shulski, M., and G. Wendler (2007), *The Climate of Alaska*, Univ. of Alaska Fairbanks, Fairbanks.
Smith, L. C., et al. (2005), Disappearing Arctic lakes, *Science*, *308*, 1429.
Turner, K. W., K. W. Turner, B. B. Wolfe, and T. W. D. Edwards (2010), Characterizing the role of hydrological processes on lake water balances in the Old Crow Flats, Yukon Territory, Canada, using water isotope tracers, *J. Hydrol.*, *386*, 103–107, doi:10.1016/j.jhydrol.2010.03.012.
Walvoord, M. A., C. I. Voss, and T. P. Wellman (2012), Influence of permafrost distribution on groundwater flow in the context of climate-driven permafrost thaw: Example from the Yukon Flats Basin, Alaska, United States, *Water Resour. Res.*, *48*, W07524, doi:10.1029/2011WR011595.
Williams, J. R. (1962), Geologic reconnaissance of the Yukon Flats district, Alaska, *U.S. Geol. Surv. Bull., 1111-H*.
Williams, J. R. (1970), Ground water in the permafrost regions of Alaska, *U.S. Geol. Surv. Prof. Pap., 696*.
Wolfe, B. B., et al. (2007), Classification of hydrological regimes of northern floodplain basins (Peace-Athabasca Delta, Canada) from analysis of stable isotopes ($\delta^{18}O$, $\delta^{2}H$) and water chemistry, *Hydrol. Processes*, *21*, 151–168.
Yoshikawa, K., and L. D. Hinzman (2003), Shrinking thermokarst ponds and groundwater dynamics in discontinuous permafrost near Council, Alaska, *Permafrost Periglacial Processes*, *14*, 151–160.

Auxiliary Material for

Controls on recent Alaskan lake changes identified from water isotopes

Lesleigh Anderson*[1], Jean Birks[2], Jennifer Rover[3], Nikki Guldager[4]

([1]U.S. Geological Survey, Geosciences and Environmental Change, Denver Colorado, USA

[2]Alberta Innovates Technology Futures, Calgary Alberta, Canada

[3]U.S. Geological Survey, Earth Resource Observation and Science (EROS), Sioux Falls South Dakota, USA

[4]Yukon Flats National Wildlife Refuge, Fairbanks Alaska, USA)

Geophysical Research Letters

Introduction:
This data set contains water isotope ratios for 175 lakes in the Yukon Flats, Alaska collected during six sampling campaigns between July 2007 and July 2011. Auxiliary text and figures (including figure captions) provides further details about the lake sampling strategy, isotope mass balance model (E/I), and source water determination. Auxiliary tables provide lake locations, isotope ratios, E/I estimates, and additional parameters with self-explanatory headings.

Table A1: Data from ten lakes sampled over multiple seasons

Lake Name	Lat (˚N)	Long (˚W)	Elev-ation (m)	Max Depth (m)[1]	Lake Area (km^2)[2]	Water-shed area (km^2)[3]	Sample Date	$\delta^{18}O$ (‰)	δ^2H (‰)	d-excess	$\Delta\delta^{18}O$ ‰	$\Delta\delta^2H$ ‰	E/I mean[4]
Twelve Mile	66.45	145.55	115	8.0	1.45	592.2	8/31/07	-7.9	-100.7	-37.53			**1.12**
							3/28/08	-8.3	-102.2	-35.51	-0.4	-1.4	1.04
							5/23/08	-8.5	-103.9	-35.54	-0.2	-1.7	1.01
							7/08/10	-7.8	-98.0	-35.60	0.7	5.9	**1.14**
							8/25/10	-7.6	-98.7	-37.86	0.2	-0.7	**1.18**
Greenpepper	66.09	146.73	201	10.0	0.87	4.38	9/1/07	-9.0	-106.4	-34.64			**0.96**
							3/26/08	-9.3	-108.2	-34.07	-0.3	-1.8	0.91
							5/27/08	-9.7	-109.3	-31.86	-0.4	-1.1	0.84
							7/24/09	-9.3	-106.0	-31.60	0.4	3.3	**0.91**
							7/23/10	-9.3	-107.1	-32.57	0.0	-1.1	**0.91**
Shack	66.30	148.11	111	1.0	0.42	7.80	8/31/07	-9.0	-106.1	-33.79			**0.96**
							3/27/08	-9.8	-112.5	-33.84	-0.3	-3.1	0.83
							5/27/08	-9.9	-112.9	-33.86	-0.1	-0.4	0.82
Scoter	66.24	146.40	130	5.0	3.27	0.746	8/31/07	-9.5	-109.4	-33.43			**0.86**
							3/27/08	-14.1	-135.2	-22.75	-1.0	-5.9	0.38
							5/27/08	-13.7	-132.8	-23.12	0.4	2.4	0.41
Teardrop	66.08	146.32	255	>10	0.35	10.66	9/1/07	-10.0	-112.2	-31.99			**0.81**
							3/27/08	-10.4	-113.8	-30.61	-0.4	-1.7	0.75
							5/23/08	-10.4	-114.2	-31.01	0.0	-0.4	0.75
Thumb	66.18	146.14	148	1.5	0.80	176.00	9/1/07	-11.7	-120.0	-26.56			**0.58**
							3/26/08	-12.4	-125.6	-26.69	-0.7	-5.6	0.48
							5/23/08	-13.9	-134.5	-23.28	-1.5	-8.9	0.34
Sands of Time	66.03	147.54	206	6.5	0.73	22.08	8/31/07	-12.9	-125.9	-22.74			**0.47**

							3/28/08	-13.3	-128.3	-22.19	-0.4	-2.4	0.44
							6/4/08	-13.8	-130.9	-20.67	-0.5	-2.6	0.40
Canvasback	66.39	146.36	124	2.5	2.79	90.95	8/31/07	-13.0	-129.3	-24.98			**0.46**
							3/27/08	-14.1	-135.2	-22.75	-1.0	-5.9	0.38
							5/27/08	-13.7	-132.8	-23.12	0.4	2.4	0.41
Twin	66.19	147.49	104	1.5	4.01	309.35	9/01/07	-14.8	-136.6	-18.45			**0.33**
							3/28/08	-14.9	-139.1	-19.78	-0.1	-2.4	0.32
							6/04/08	-19.2	-161.3	-7.58	-4.3	-22.2	0.10
West Crazy	65.93	146.60	293	6.4	0.64	69.58	9/1/07	-16.5	-144.4	-12.45			**0.23**
							3/27/08	-16.7	-147.2	-13.23	-0.3	-2.8	0.22
							5/23/08	-18.5	-157.7	-9.72	-1.8	-10.6	0.14

[1]Measured in 2007
[2]Derived from imagery obtained between 2008-2011
[3]Estimated from 10-m DEM
[4]Calculated with 1979-2011 climate mean, bolded values show late summer values compared in the text

Table A2: Data for 175 lakes

Lake ID	Day-Month	Year	Lat (˚N)	Long (˚W)	Elevation (m)	$\delta^{18}O$ (VSMOW)	$\delta^{2}H$ (VSMOW)	E/I	Specific Conductance (µS/cm)	Source (2=snow/ permafrost)	Trend (1=dec, 2=nc, 3=inc)
12 Mile Lake	30-Aug	2007	66.450	-145.546	115	-7.90	-100.73	1.12	552		1
12 Mile Pond	30-Aug	2007	66.450	-145.563	115	-4.46	-84.94	2.24	1425		
Canvasback	30-Aug	2007	66.385	-146.360	124	-13.04	-129.30	0.46	609		2
Sands of Time	30-Aug	2007	66.034	-147.544	207	-12.89	-125.86	0.47	143		
Shack	30-Aug	2007	66.294	-148.114	111	-9.04	-106.11	0.96	1423		
Greenpepper	31-Aug	2007	66.088	-146.733	202	-8.97	-106.40	0.96	831		1
Scoter	31-Aug	2007	66.240	-146.394	130	-9.49	-109.35	0.86	320		2
Teardrops	31-Aug	2007	66.083	-146.316	255	-10.02	-112.15	0.81	232		2
Thumb	31-Aug	2007	66.175	-146.144	148	-11.68	-120.00	0.58	126		2
Twin	31-Aug	2007	66.186	-147.493	104	-14.77	-136.61	0.33	145		2
West Crazy	31-Aug	2007	65.929	-146.596	293	-16.49	-144.37	0.23	119		
252A	9-Jul	2008	66.129	-146.660	198	-10.50	-116.86	0.73	206.6		1
51A	10-Jul	2008	66.282	-149.321	110	-18.00	-155.82	0.15	127.6		
83A	10-Jul	2008	66.259	-148.935	103	-9.98	-111.39	0.83	169.3		
86A	10-Jul	2008	66.337	-148.984	115	-15.14	-141.79	0.30	184.3		
91A	10-Jul	2008	66.240	-148.825	100	-15.22	-142.46	0.30	167.3		
231A	15-Jul	2008	66.229	-146.943	117	-17.59	-150.50	0.17	72.6		2
255A	15-Jul	2008	66.223	-146.688	119	-9.91	-116.08	0.80	199.6		1
281A	15-Jul	2008	66.217	-146.417	126	-13.58	-135.62	0.41	204.2		2
281B	15-Jul	2008	66.217	-146.385	128	-10.54	-118.78	0.71	318.6		2
292A	15-Jul	2008	66.258	-146.331	118	-8.77	-112.11	0.97	700		2
295A	15-Jul	2008	66.320	-146.320	128	-10.52	-116.84	0.72	521.6		2
306A	15-Jul	2008	66.299	-146.187	130	-12.00	-127.86	0.55	405.9		
129A	16-Jul	2008	66.106	-148.220	106	-18.29	-158.00	0.14	159.9		
151A	16-Jul	2008	66.171	-147.975	107	-9.17	-109.27	0.93	273		
174A	16-Jul	2008	66.208	-147.669	108	-18.21	-156.04	0.14	193		
43A	16-Jul	2008	66.067	-149.327	92	-11.20	-121.94	0.64	169.5		
69A	16-Jul	2008	66.117	-149.069	105	-14.50	-139.92	0.34	78.5		
97A	16-Jul	2008	66.200	-148.682	97	-7.76	-104.12	1.26	236.9		

157A	16-Jul	2008	66.459	-147.903	132	-9.13	-111.44	0.97	215.7		2
187A	16-Jul	2008	66.389	-147.573	112	-8.40	-105.14	1.10	435		2
193A	16-Jul	2008	66.430	-147.412	114	-7.37	-103.30	1.36	196.8		1
276A	22-Jul	2008	66.055	-146.384	222	-17.43	-152.56	0.19	120.3		2
332A	22-Jul	2008	66.061	-145.782	220	-14.16	-137.52	0.38	189.5		2
349A	22-Jul	2008	66.187	-145.668	134	-13.72	-136.30	0.40	200.4		2
350A	22-Jul	2008	66.207	-145.658	136	-18.51	-158.26	0.14	167.9		2
353A	22-Jul	2008	66.277	-145.708	131	-18.70	-158.91	0.13	132.1		2
360A	22-Jul	2008	66.110	-145.561	201	-14.53	-139.24	0.35	184.3		
365A	22-Jul	2008	66.368	-145.562	134	-11.48	-122.97	0.60	489.3		2
374A	22-Jul	2008	66.185	-145.444	143	-18.85	-153.56	0.12	154		
EX1	22-Jul	2008	66.010	-146.444	248	-15.41	-143.52	0.29	143.2		
EX2	22-Jul	2008	65.999	-146.468	230	-18.63	-156.95	0.13	120		
110A	25-Jul	2008	66.281	-148.593	102	-10.44	-117.81	0.75	343.4		
112A	25-Jul	2008	66.327	-148.595	102	-12.87	-130.87	0.48	193.4		
134A	25-Jul	2008	66.275	-148.221	110	-9.70	-115.61	0.85	734		
145A	25-Jul	2008	66.307	-148.102	109	-10.03	-115.81	0.80	1392		
145B	25-Jul	2008	66.314	-148.106	106	-10.30	-118.18	0.76	1450		
145C	25-Jul	2008	66.280	-148.120	101	-10.18	-115.71	0.77	1164		
398	15-Jul	2009	66.123	-148.153	105	-11.30	-120.90	0.62	131.2		
234	15-Jul	2009	66.131	-149.159	99	-18.80	-156.90	0.12	88.5		
270	15-Jul	2009	65.971	-149.450	129	-16.90	-162.50	0.38	50.9	2	
74	15-Jul	2009	66.167	-149.159	93	-11.60	-128.70	0.59	191.7		
182	15-Jul	2009	66.260	-148.878	100	-17.30	-165.70	0.36	186.8	2	
458	15-Jul	2009	66.179	-148.989	99	-7.40	-105.50	1.44	273.3		
189	16-Jul	2009	66.106	-147.554	177	-10.40	-110.00	0.75	402.2		
2 SPAT	16-Jul	2009	66.110	-147.753	184	-13.20	-125.00	0.45	224.7		
445	16-Jul	2009	66.150	-147.731	111	-11.90	-139.00	0.99	174.3	2	
227	16-Jul	2009	66.181	-148.010	0	-9.20	-105.00	0.88	239.9		
606	16-Jul	2009	66.110	-148.313	105	-16.10	-153.00	0.45	155.7	2	
251	21-Jul	2009	66.993	-146.169	165	-16.70	-149.00	0.24	144		2
187	21-Jul	2009	66.983	-146.041	162	-10.30	-119.00	0.79	433		2
507	21-Jul	2009	66.928	-146.125	160	-10.70	-117.00	0.73	223		2
599	21-Jul	2009	66.783	-145.799	134	-19.10	-160.00	0.13	190		2
427	22-Jul	2009	66.909	-145.113	147	-10.40	-113.00	0.75	417		2
171	22-Jul	2009	66.897	-145.170	145	-10.50	-115.00	0.74	370		2
159 (Track)	22-Jul	2009	66.856	-145.170	145	-7.20	-99.00	1.29	600		2

287	22-Jul	2009	66.775	-145.258	140	-7.30	-98.00	1.29	881		2
331	22-Jul	2009	66.751	-145.458	142	-12.90	-127.00	0.49	534		2
395	22-Jul	2009	66.707	-145.530	134	-12.10	-124.00	0.56	224		2
456	24-Jul	2009	66.154	-144.118	177	-16.70	-145.00	0.23	153		
127	24-Jul	2009	66.752	-143.502	174	-14.50	-137.00	0.37	189		
84	24-Jul	2009	66.716	-143.673	162	-10.50	-116.00	0.74	216		
136	24-Jul	2009	66.444	-144.384	144	-18.90	-157.00	0.13	124		
332	24-Jul	2009	66.418	-145.368	138	-10.80	-119.00	0.68	374		2
112 SPAT	31-Aug	2009	66.101	-146.007	239	-7.80	-113.60	2.27	166	2	1
33	31-Aug	2009	66.625	-146.234	127	-7.90	-113.60	2.24	467	2	2
44	31-Aug	2009	66.269	-145.902	132	-7.80	-118.40	2.13	413	2	2
4	31-Aug	2009	66.867	-143.837	158	-6.80	-114.60	2.85	745	2	
4 SPAT	31-Aug	2009	66.871	-143.829	159	-8.00	-117.60	2.15	985	2	
68	31-Aug	2009	66.995	-143.749	185	-10.30	-129.90	1.36	3995	2	
63 Alt	31-Aug	2009	66.977	-143.327	173	-13.70	-146.30	0.74	528	2	
148	31-Aug	2009	66.796	-143.538	169	-8.30	-116.70	1.95	1847	2	
8	31-Aug	2009	66.657	-143.839	161	-8.60	-121.30	1.80	196	2	
47	1-Sep	2009	66.640	-145.301	135	-10.30	-138.40	1.28	623	2	2
55	1-Sep	2009	66.850	-145.552	152	-5.00	-103.70	4.93	357	2	2
1 SPAT	1-Sep	2009	66.754	-146.679	155	-11.80	-139.30	1.04	340	2	2
87	1-Sep	2009	66.834	-145.880	135	-7.90	-118.30	2.28	272	2	2
17	1-Sep	2009	66.612	-146.668	129	-9.00	-121.90	1.78	825	2	1
81	1-Sep	2009	66.547	-146.636	117	-12.70	-146.60	0.85	417	2	2
73	1-Sep	2009	66.440	-146.545	117	-11.80	-138.90	1.02	533	2	2
41	1-Sep	2009	66.335	-146.842	116	-10.60	-135.10	1.30	562	2	1
29	1-Sep	2009	66.244	-146.610	123	-6.90	-112.20	3.18	370	2	2
31	15-Sep	2009	66.592	-144.865	143	-6.80	-105.00	1.39	257		
399	15-Sep	2009	66.654	-144.481	146	-15.30	-151.00	0.54	181	2	
116 Alt	15-Sep	2009	66.633	-144.320	144	-7.60	-107.00	1.20	688		
164	15-Sep	2009	66.705	-144.009	156	-8.20	-108.00	1.09	222		
356	15-Sep	2009	66.782	-144.001	159	-17.80	-154.00	0.18	160		
50	15-Sep	2009	66.802	-144.395	154	-8.40	-112.00	1.06	198		
292	15-Sep	2009	66.043	-149.557	132	-6.40	-101.00	1.99	290		
14 SPAT	18-Sep	2009	66.045	-149.569	137	-14.00	-144.00	0.69	93	2	
14	18-Sep	2009	66.185	-149.420	104	-14.00	-140.00	0.38	256		
26	18-Sep	2009	66.216	-149.130	102	-13.80	-142.00	0.39	55		
10	18-Sep	2009	66.301	-148.459	107	-12.60	-133.00	0.50	247		

110	18-Sep	2009	66.233	-147.665	106	-9.20	-117.00	0.92	390		1
22	18-Sep	2009	66.269	-147.247	107	-9.30	-111.00	0.91	660		1
61	18-Sep	2009	66.090	-147.162	212	-12.60	-134.00	0.50	618		
41 Alt	18-Sep	2009	66.316	-146.840	108	-9.40	-121.00	1.68	3397	2	1
MUD 2	18-Sep	2009	66.310	-146.906	116	-9.30	-121.00	1.72	2722	2	1
Goblin Pond	20-Jul	2010	66.401	-146.384	122	-8.44	-104.57	1.05			3
Habanero Pond	25-Jul	2010	66.087	-146.729	206	-13.78	-130.33	0.40			
12Mile #2	27-Jul	2010	66.440	-145.477	137	-6.95	-98.55	1.36			2
12Mile #1	27-Jul	2010	66.437	-145.479	136	-6.74	-100.34	1.41			2
Piddle Pond	28-Jul	2010	66.431	-145.536	134	-5.61	-98.87	1.75			1
C4	5-Jul	2011	66.391	-148.325	118	-15.87	-145.37	0.27			
C6	2-Jul	2011	66.386	-148.344	112	-8.48	-110.57	1.09			
C7	3-Jul	2011	66.385	-148.328	111	-15.87	-146.01	0.27			
C8	5-Jul	2011	66.386	-148.321	117	-17.16	-149.19	0.20			
C9	4-Jul	2011	66.387	-148.304	118	-7.66	-107.94	1.29			
C10	4-Jul	2011	66.386	-148.290	115	-8.05	-106.63	1.18			
C11	3-Jul	2011	66.383	-148.317	113	-15.51	-144.20	0.29			
C12	2-Jul	2011	66.384	-148.350	110	-10.91	-126.72	0.69			
C13	2-Jul	2011	66.383	-148.355	109	-6.93	-106.47	1.50			
C16	2-Jul	2011	66.376	-148.348	106	-12.11	-125.30	0.55			
C18	1-Jul	2011	66.371	-148.312	110	-10.17	-115.23	0.78			
C19	3-Jul	2011	66.373	-148.350	106	-11.68	-124.20	0.59			
C22	1-Jul	2011	66.367	-148.324	111	-12.03	-126.97	0.56			
C23	4-Jul	2011	66.388	-148.298	118	-6.68	-106.88	1.59			
D1	13-Jul	2011	66.120	-148.048	104	-9.15	-106.96	0.93			
D2	11-Jul	2011	66.106	-148.076	105	-12.98	-131.12	0.45			
D4	9-Jul	2011	66.109	-148.089	104	-19.29	-158.25	0.10			
D6	13-Jul	2011	66.111	-148.050	105	-19.91	-160.80	0.08			
D7	12-Jul	2011	66.109	-148.056	105	-16.01	-143.73	0.25			
D11	9-Jul	2011	66.106	-148.089	104	-18.68	-155.32	0.12			
D12	12-Jul	2011	66.105	-148.071	105	-12.31	-131.50	0.51			
D13	11-Jul	2011	66.105	-148.056	105	-18.20	-154.12	0.14			
D14	10-Jul	2011	66.101	-148.097	104	-17.05	-149.82	0.19			
D15	8-Jul	2011	66.102	-148.093	104	-18.53	-154.64	0.13			
D18	11-Jul	2011	66.102	-148.079	104	-13.04	-132.20	0.45			
D23	10-Jul	2011	66.100	-148.100	104	-17.59	-150.68	0.17			
D35	8-Jul	2011	66.091	-148.077	105	-13.61	-131.44	0.40			

D24	10-Jul	2011	66.098	-148.097	104	-19.32	-158.10	0.10
D26	8-Jul	2011	66.100	-148.090	104	-17.72	-151.41	0.16
D27	9-Jul	2011	66.097	-148.087	105	-17.95	-151.18	0.15
D34	8-Jul	2011	66.093	-148.057	107	-17.33	-150.48	0.18
D38	13-Jul	2011	66.119	-148.063	104	-11.03	-119.80	0.65
L5	5-Jul	2011	66.030	-144.742	163	-11.06	-120.61	0.64
L6	5-Jul	2011	66.029	-144.737	163	-15.21	-141.09	0.30
L13	5-Jul	2011	66.026	-144.727	163	-16.08	-143.84	0.25
L16	6-Jul	2011	66.015	-144.728	162	-19.66	-152.93	0.09
L19	2-Jul	2011	66.017	-144.780	165	-11.84	-124.03	0.56
L21	2-Jul	2011	66.015	-144.769	164	-13.85	-133.63	0.39
L22	2-Jul	2011	66.013	-144.773	165	-12.13	-124.71	0.53
L23	4-Jul	2011	66.012	-144.781	165	-13.64	-132.99	0.41
L24	4-Jul	2011	66.010	-144.783	165	-9.16	-112.63	0.89
L26	1-Jul	2011	66.010	-144.759	165	-15.09	-138.96	0.31
L27	6-Jul	2011	66.014	-144.739	163	-16.66	-144.47	0.22
L28	4-Jul	2011	66.006	-144.769	165	-11.05	-121.14	0.64
L29	3-Jul	2011	66.008	-144.743	164	-15.38	-141.68	0.29
L30	3-Jul	2011	66.008	-144.739	164	-16.78	-147.14	0.22
L31	3-Jul	2011	66.007	-144.735	164	-19.03	-151.79	0.11
L60	1-Jul	2011	66.011	-144.748	163	-15.33	-140.60	0.30
M25	8-Jul	2011	66.359	-144.268	156	-7.23	-102.70	1.33
M20	9-Jul	2011	66.364	-144.253	156	-8.86	-108.58	0.98
M22	11-Jul	2011	66.361	-144.265	156	-13.94	-131.38	0.40
M24	9-Jul	2011	66.366	-144.233	157	-17.14	-139.55	0.21
M27	10-Jul	2011	66.359	-144.237	157	-13.09	-129.97	0.47
M28	10-Jul	2011	66.362	-144.225	157	-7.06	-101.11	1.38
M37	10-Jul	2011	66.355	-144.232	157	-11.29	-122.05	0.64
M49	11-Jul	2011	66.358	-144.250	157	-15.52	-142.31	0.29
M51	11-Jul	2011	66.359	-144.241	157	-14.83	-136.58	0.34
H11	21-Jul	2011	66.400	-146.371	117	-8.68	-106.50	1.00
H13	22-Jul	2011	66.397	-146.409	118	-11.73	-126.31	0.58
H14	21-Jul	2011	66.396	-146.355	119	-10.13	-117.17	0.77
H16	21-Jul	2011	66.386	-146.367	117	-8.33	-103.76	1.07

Anderson, Birks, Rover, Guldager – Alaska lake change from water isotopes
Auxiliary Figure 1

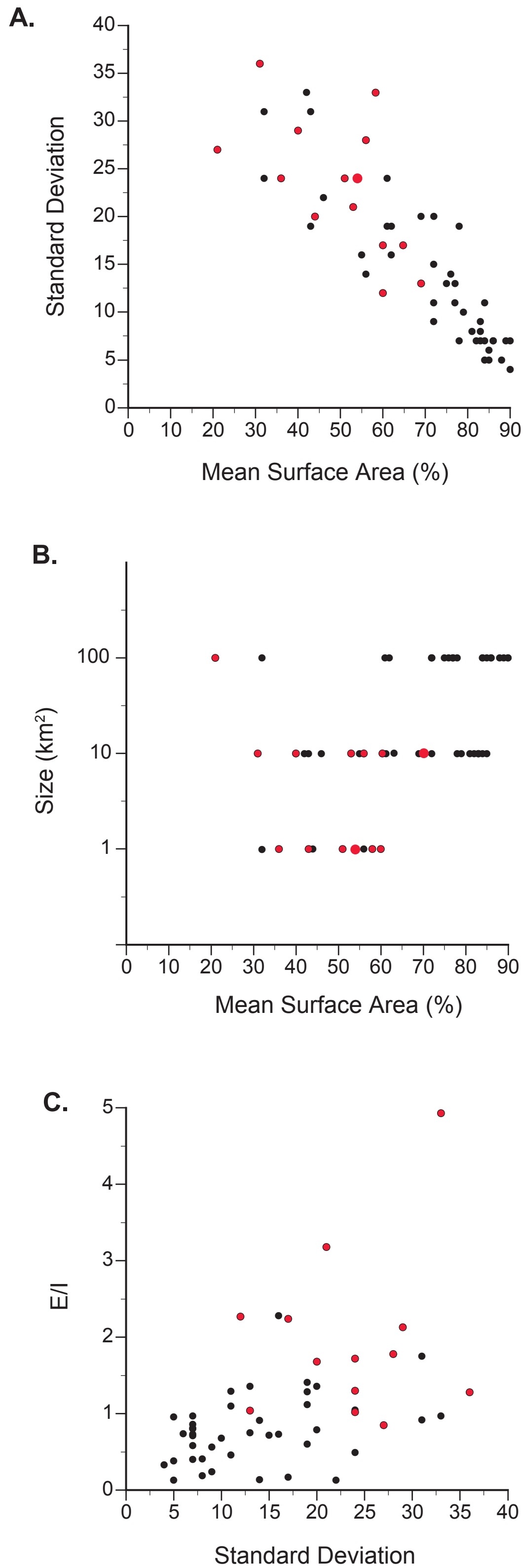

Anderson, Birks, Rover, Guldager – Alaska lake change from water isotopes

Auxiliary Fig. 2

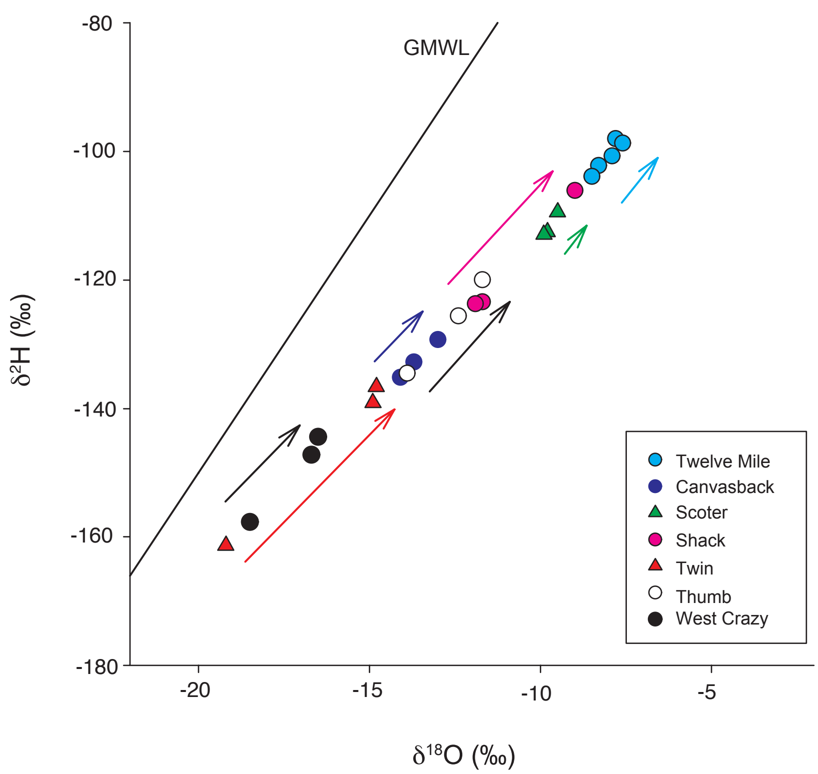

Auxiliary Fig. 3

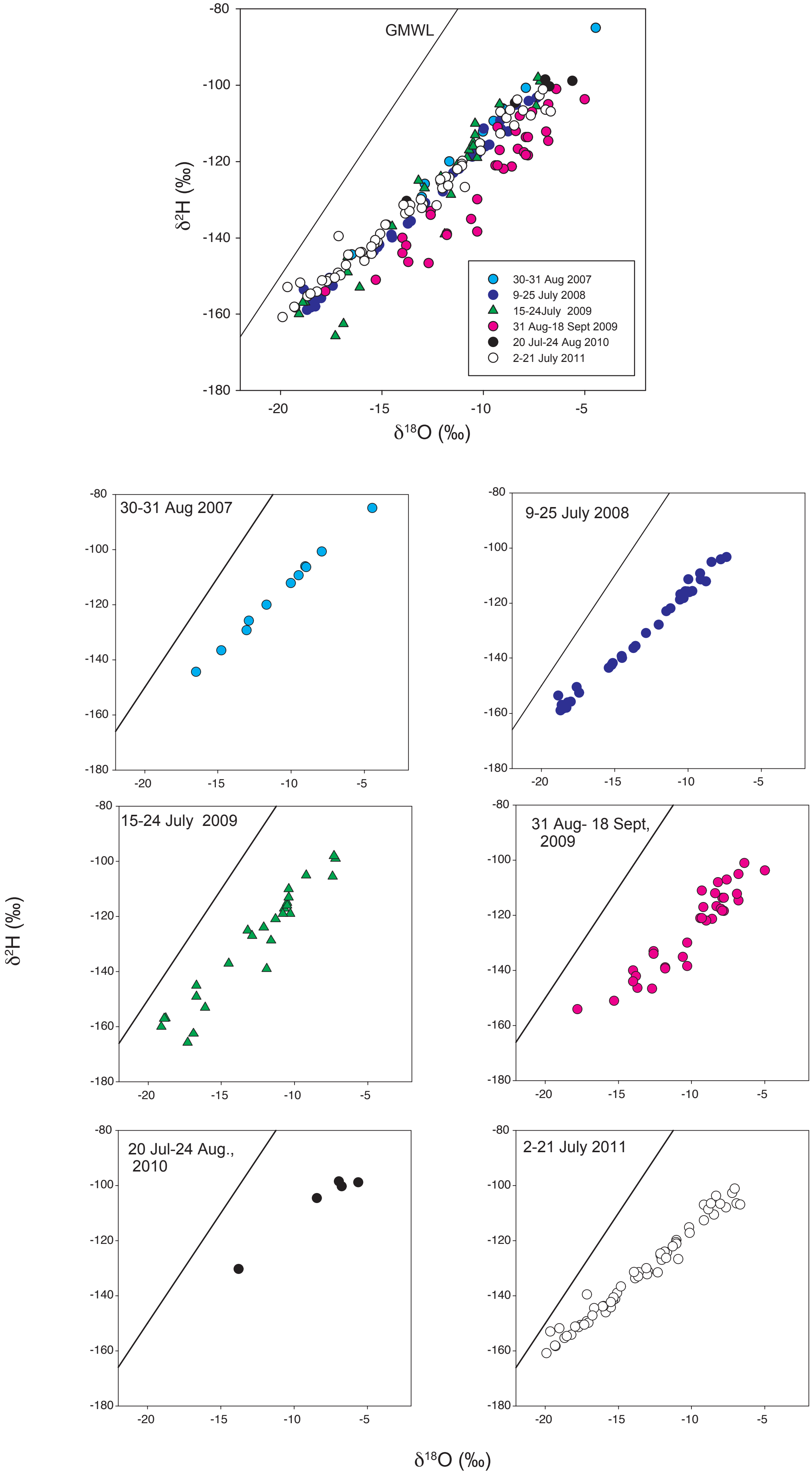

Auxiliary Fig. 4

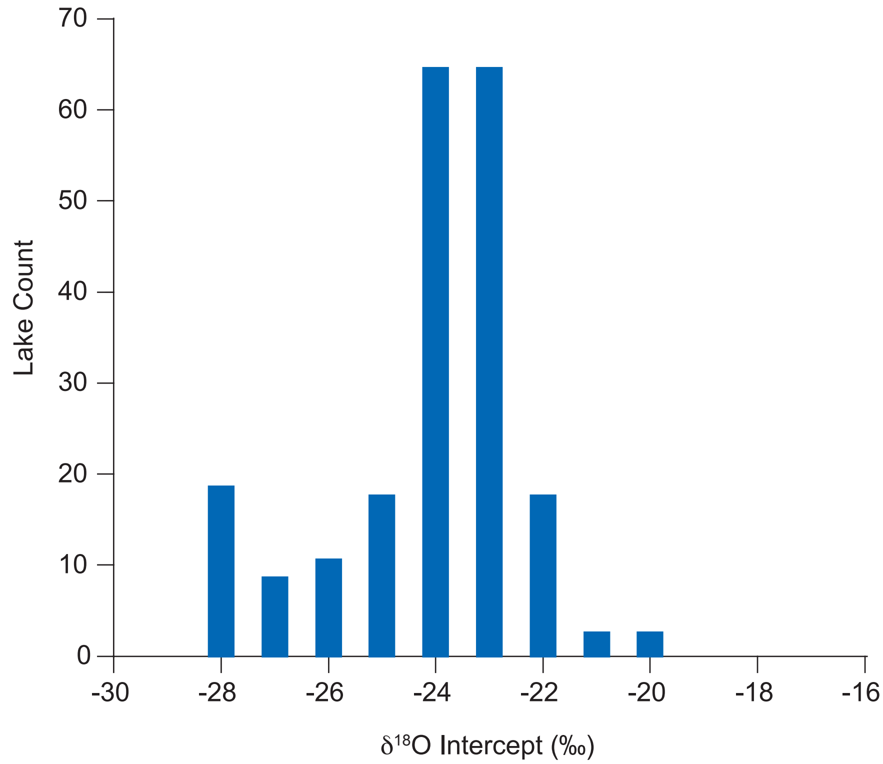

Auxiliary Fig. 5

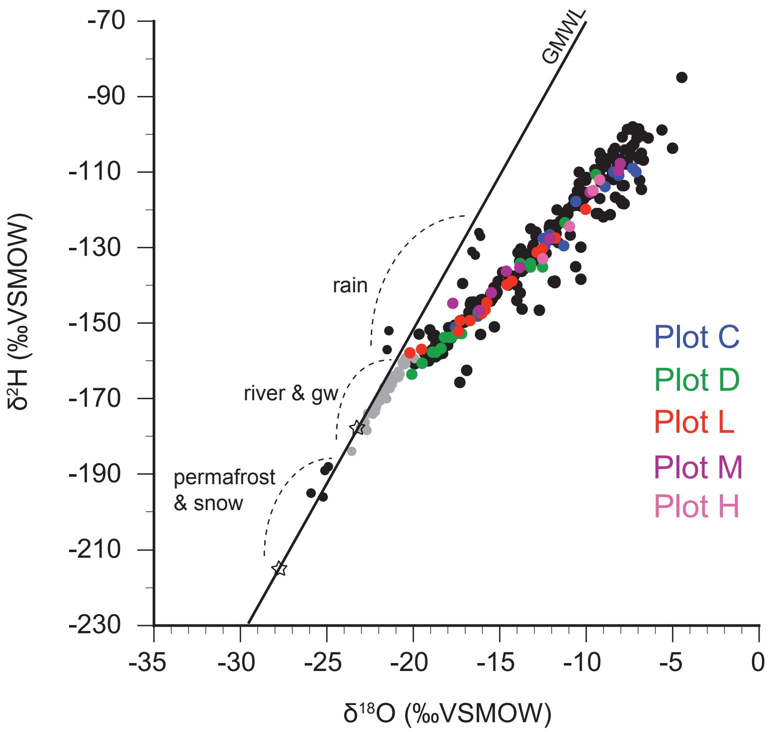

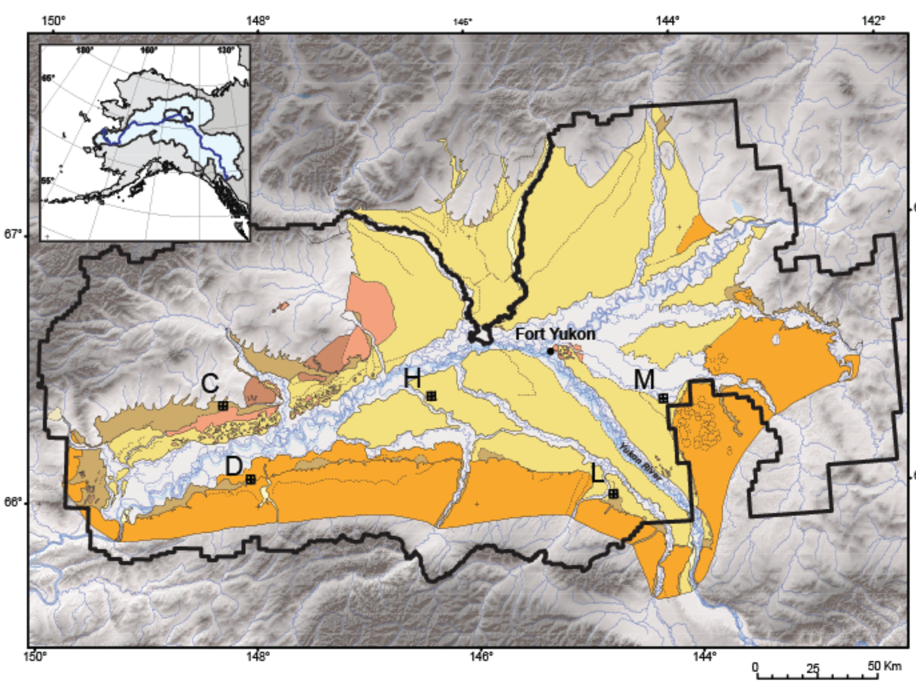

Auxiliary Text:

Lake sampling strategy

Five strata were delineated within the Yukon Flats area that include all wetlands within the National Wildlife Refuge, and are based on natural divisions in topography and hydrology (Fig.1). Wetlands within each strata were randomly selected utilizing a Generalized Random Tessellation Stratified **(**GRTS) design in Arc Geographic Information System (GIS) that allows for spatially balanced random sampling [*Stevens and Olsen*, 2004]. Wetlands were selected from a polygon shape file of water-body extent derived from year 2000 Landsat Thematic Mapper satellite image mosaics. The South Flats stratum includes wetlands south of the Yukon River below 500 ft elevation, and includes lower Beaver and lower Birch Creeks. The South Hills stratum includes deeper lakes that lie at higher elevations (> 500 ft) along the north slope of the White Mountains and includes upper Beaver Creek. The North stratum lies north of the Yukon River, and includes the lower portions of the Chandalar and Christian rivers. The West stratum includes wetlands within the western portion of the Yukon Flats and lies north of the Yukon River. The East stratum is located in eastern Yukon Flats and includes lower portions of the Sheenjek, Porcupine, Black and Little Black Rivers.

E/I Calculations

1. Isotope Mass Balance Model

An isotope mass balance (IMB) model was used to assess lake water balance, including the ratio of evaporation to inflow (E/I), for the 175 lakes. The IMB model determines flushing rates for each lake based on the degree of offset between measured lake water $\delta^{18}O$ and $\delta^{2}H$ and estimated isotope composition of precipitation at each site. Application of lake IMB modeling has previously been shown to be useful for quantifying site specific estimates of hydrology from regional lake surveys in un-gauged and under monitored catchments.

In hydrologic and isotopic steady-state, water and isotope balances for a typical lake are expressed, respectively as:

$$[1] \quad I = Q + E$$

$$[2] \quad I\,\delta_I = Q\delta_Q + E\delta_E$$

Here, I is the inflow rate (m^3s^{-1}), Q is the outflow rate (m^3s^{-1}) and E is the evaporation rate (m^3s^{-1}). δ_I, δ_Q *and* δ_E each represent the isotopic composition of each corresponding hydrological component. These equations can be simplified using the general assumptions that outflow from the lake is equivalent to lake water ($\delta_Q = \delta_L$) and that inflows can be approximated by the weighted annual average of precipitation ($\delta_I = \delta_P$). The Craig-Gordon Model for open water evaporation [*Craig and Gordon*, 1965] is used to estimate ™$_E$:

$$[3] \quad \delta_E = \alpha^* \,\delta_L - h\,\delta_A - \Sigma^* - h + \Sigma_K$$

Here, 〈* is the equilibrium fractionation between liquid and vapor (Σ^*=〈*-1), and Σ is the total enrichment factor including both equilibrium (Σ^*) and kinetic (Σ_K) components. Combining and rearranging these equations yields an expression for the fraction of water loss by evaporation, E/I, expressed as:

$$[4] \quad E/I \approx (\delta_L - \delta_P) / m\,(\delta^* - \delta_L)$$

Here, m is the enrichment slope derived from $(h - \Sigma) / (1 - h + \Sigma_K)$ where h is humidity (relative humidity/100), and $\delta^* = (h\,\delta_A + \Sigma) / (h - \Sigma)$ is the limiting isotopic enrichment. Values for Σ^* were estimated using temperature data and the equations from *Horita and Wesolowski* [1994]. Estimates of Σ_K were determined using relative humidity using $\Sigma_K = C_K(1-h)$ where C_K was set to 14.2 ‰ for oxygen and 12.5 ‰ for hydrogen [*Gibson et al.*, 2002]. The isotopic composition of atmospheric moisture, ™$_A$, was determined using a similar method as *Bennett et al.*, [2008]; *Gibson et al.*, [2008] and *Gibson et al.*, [2010a], and [2010b], starting with the equilibrium assumption ($\delta_A = \delta_p - k\,\Sigma^*$, $k=1$) and then iteratively adjusting k to obtain a best-fit match for $\delta^{18}O$ and δ^2H results by best fitting k to the observed local evaporation line.

In this study, equation [4] was used to determine E/I values from measured lake $\delta^{18}O$ and $\delta^{2}H$ compositions from the surveys conducted between 2007 and 2011 using climatological averages from gridded climate datasets. The results of the E/I calculations from $\delta^{18}O$ are presented in this report but they are highly correlated with the E/I results from $\delta^{2}H$ (r^2=0.9486), and similar trends were found for those calculations.

2. Climate Parameters

In the absence of a network of long-term, reliable meteorological stations within the ~118,340 km^2 Yukon Flats region, climatological parameters required to run the IMB were obtained from the North American Regional Reanalysis (NARR) dataset [*Mesinger et al.,* 2006]. The NARR dataset is a long-term, dynamically consistent, high-resolution, high frequency, atmospheric and land surface hydrology dataset for the North American domain based on meteorological station data between 1979 and 2003. Average monthly climate fields (*i.e.*, climate norms) were extracted for the grid cells corresponding to the location of each of the 175 lakes in the survey. The parameters extracted were:

APCPsfc: surface total precipitation [kg/m^2]
RH2m: 2 m relative humidity [%]
EVPsfc: surface evaporation [kg/m^2]
TMP2m: 2 m temp. [K]

Climate data from the time period corresponding to the residence time of the lake would give the best representation of climate conditions during lake evaporation, but climate norms are often used in regional lake surveys where a wide variety of residence times might be expected [*e.g. Bennett et al.,* 2008, *Gibson and Edwards,* 2002, *Gibson et al.,* 2010a, 2010b, *Pham et al.,* 2008, and *Scott et al.,* 2010]. The interannual variations observed between 2007 and 2010 are indicated by the following ranges of deviation from long-term climate norms: ΔT=-0.2°C to +1.5°C; ΔRH, -2.4 % to -4.7%; ΔP= -4.6 to 2.0 mm/mo.

The evaporation flux-weighting approach developed by *Gibson et al.* [2002] was used to flux-weight (FW) estimates of relative humidity and temperature so that the water balance calculations are representative of the open water season. For example the evaporation flux-weighted estimates for 2m temperature over a year (T_{FW}) is given below as the sum of the temperature *(T)* multiplied by the evaporation (*E)* for each month divided by the sum of the total evaporation over 12 months ($T_{FW} = \sum E_{monthly}\, T_{monthly} / \sum E_{annual}$)

Monthly precipitation $\delta^{18}O$ estimates were obtained for each lake location based on empirically derived relationships between latitude and elevation presented by *Bowen and Wilkinson* [2002] and tuned/corrected using available Canadian Network for Isotopes in Precipitation (CNIP) data. The ™^{2}H was calculated assuming that precipitation would follow the relationship defined by the Global Meteoric Water Line (GMWL) [*Craig*, 1961]. However, rather than flux weighting, amount weighting precipitation *(P_{AW})* best represents monthly precipitation isotope fields *(δ_P)*. Using precipitation from the NARR data set, the average precipitation total for each month *(P)* is multiplied by the estimated ™$_p$ for that month, divided by the precipitation total over 12 months ($\delta_{PAW} = \sum \delta_{p\text{-}monthly}\, P_{monthly} / \sum P_{annual}$).

3. Isotope Mass Balance Model Assumptions

The major assumptions inherent in the IMB approach include that:

(i) The isotopic composition of atmospheric moisture is a function of the isotopic composition of precipitation, as is expected due to near-equilibrium exchange between vapor and liquid water in condensing air masses,

(ii) The isotopic composition of discharge is adequately characterized by the isotopic signature of lake water (™$_L$) expected for a well-mixed lake,

(iii) The isotopic composition of inflow to the lake is equal to that of precipitation (*i.e.* ™$_I$ = ™$_P$), as would be valid where runoff is locally derived from recent meteoric water that has not undergone substantial isotopic enrichment, and

(iv) Lake samples collected during summer/early fall are sufficiently representative of the annual long-term isotopic composition of the lake to evaluate the proposed hypothesis.

The first three assumptions are clearly valid for the Yukon Flats lake dataset. First, there are no isotopically distinct vapor sources (e.g. large lakes or near ocean) or strong evidence for mixing with transpired vapor. Second, the sampled sites did not include very large, deep lakes with permanent stratification that would differentiate outflow from lake water isotope values. Third, the similarity between precipitation and surface run-off isotope values is evident by the similarity between Yukon River water data and integrated precipitation.

To address the fourth assumption, temporal trends in the isotopic composition of a subset of lakes that were sampled multiple times during the study period are more closely examined (Table A1 and Fig. A2). The available data show the most negative δ^{18}O and δ^{2}H values occur after spring melt, followed by evaporative enrichment over the open water period. The greatest change in lake water isotopes, and corresponding E/I, occurred during the period between spring melt and early summer and significantly less change occurred during the July to September period. It is possible that E/I estimates based on early to mid July samples may slightly underestimate evaporation, but this effect would have limited impact on the overall range of E/I (Table A2). Therefore, we have combined all isotope data obtained between mid-July through early September for our analyses.

Furthermore, because our purpose here is to evaluate the overall range of hydrologic states in the study area, we also combined the mid to late summer data for all of the five years during which sampling campaigns were conducted (2007-2011). This approach is validated by comparing the data for each sampling campaign (Fig. A3) which shows that the range of all the isotope values (max – min = ~15‰) is similar from one year to the next, and far greater than the largest observed seasonal change at an individual site. These results are similar to the spatial and temporal variations observed by other regional lake surveys including the Old Crow Flats, northern Yukon Territory [*Turner et al.*, 2010] that is the nearest available data set to the Yukon Flats. There also, the greatest difference in isotopes and E/I estimates occurs between ice-out and early summer. The overall range of the entire data set is also similar from year to year and exceeds individual lake seasonal variations.

5. Source water evaluation

Visibly evident within the ™^{18}O and ™^{2}H scatter plot are two groups of lakes (Fig. 3) that appear to be defined by regressions (local evaporation lines, LEL) with similar slopes but different intercepts on the GMWL. More specifically, when inflow

(™$_I$) was estimated using precipitation *(™$_p$)* based on the geographical position of the lake, the LEL regression between some of the lakes *(™$_L$)* and the ™$_p$ value produced unrealistically low slopes (m = 1 to 3) compared with slopes that are either theoretically predicted or observed in similar areas (m ≈ 4.5 to 5.5). This suggested that assumption (iii), where ™$_I$ approximates ™$_p$, should be re-evaluated for this group of lakes.

Here we use the constant local evaporation line (LEL) approach, with a slope of 5, to derive the intercepts with the GMWL for all lakes [*e.g., Wolfe et al.,* 2007]. A slope of 5 is slightly higher than the empirically derived slope of 4.6 from the dataset, yet it is similar to slopes derived from other high latitude lake surveys [*Gibson et al.,* 2005]. Fitting an LEL with a slope of 5 to each of the lake data points identified a range of intercept values on the GMWL between -30 and -20‰ for ™^{18}O and a bi-modal distribution (Fig. A4). The majority of lakes (n= 124) plot on the LEL that intercepts the GMWL at -24‰ ± 1‰. A small group (n=26) plots on the LEL that intercepts the GMWL at -28‰ ± 1‰. Therefore, the source water, ™$_I$, used to estimate E/I for these 26 lakes was ~4‰ more negative than the expected ™$_p$, allowing some variance related to elevation and latitude. Although further refinement of ™$_I$ may be possible by coupling the E/I estimates with both ™^{18}O and ™^{2}H following the method of Yi et al., [2008], this approach is not necessary in order to determine the existence of two groups, one sourced by water relatively enriched in O^{18}, and the other relatively depleted.

References:

Bennett, K.E. et al., (2008). Water Yield estimates for critical loadings assessment: comparisons of gauging methods versus and isotopic approach. *Can. J. Fish. Aquat. Sci.* 65: 83-99.

Bowen, G.J., & B. Wilkinson. (2002). Spatial distribution of d^{18}O in meteoric precipitation. *Geology,* 30:315-318.

Craig, H. (1961). Isotopic variations in meteoric waters. *Science,* 133:1702-1703.

Craig, H., and L. I. Gordon (1965), *Deuterium and oxygen-18 variation in the ocean and the marine atmosphere,* Proc. Conf. on Stable Isotopes in Oceanographic Studies and Paleotemperatures, ed: E. Tongiorgi, pp. 9-130, Spoleto, Italy.

Gibson, J.J., et al., (2005). Progress in isotope hydrology in Canada. *Hydrol. Proc*. 19, 303-327.

Gibson, J.J., et al., (2002). Quantitative comparison of lake throughflow, residency, and catchment runoff using stable isotopes: modeling and results from a regional survey of Boreal lakes. *J. Hydrol.* 262: 128-144.

Gibson, J.J. et al., (2010a) Interannual variations in water yield to lakes in northeastern Alberta: Implications for estimating critical loads of acidity. *J. Limnol.,* 69(Suppl. 1): 126-134.

Gibson, J.J. et al., (2010b) Site-specific estimates of water yield applied in regional acid sensitivity. *J. Limnol.,* 69 (Suppl. 1): 67-76

Scott, K.A. et al., (2010) Limnological characteristics and acid sensitivity of boreal headwater lakes in northwest Saskatchewan, Canada. *J. Limnol*., 69 (Suppl. 1): 33-44.

Horita, J., and D. Wesolowski (1994), Liquid-vapour fractionation of oxygen and hydrogen isotopes of water from the freezing to the critical temperature, *Geochim. Cosmochim. Acta.,* 58, 3425-3437.

Stevens, D. L. and Olsen, A. R. 2004. Spatially balanced sampling of natural resources. *J. Amer. Stat. Assoc.* 99, 262 – 278.

Turner, K.W. et al., (2010). Characterizing the role of hydrologic processes on lake water balances in the Old Crow Flats, Yukon Territory, Canada, using water isotope tracers. *J. Hydrol.,* 386, 103-117.

Mesinger F. et al., (2006). North American Regional Reanalysis: A long-term, consistent, high-resolution climate dataset for the North American domain, as a major improvement upon the earlier global reanalysis datasets in both resolution and accuracy. *Bull. Amer .Meteorol. Soc.,* 87: 343-360.

Pham, S. V. et al., (2008). Spatial variability of climate and land-use effects on lakes of the northern Great Plains, Limnology and Oceanography, 53(2), 728-742, doi: 10.4319/lo.2008.53.2.0728.

Wolfe, B.B. et al., (2007). Classification of hydrological regimes of northern floodplain basins (Peace-Athabasca Delta, Canada) from analysis of stable isotopes (™^{18}O, ™^{2}H) and water chemistry. *Hydrol*. Proc. 21, 151-168.

Yi, Y. et al., (2008). A coupled isotope tracer method to characterize input water to lakes. *J. Hydrol.* 35, 1-13.

Auxiliary Figure Captions

Figure A1. Data from 54 lakes that were analyzed for surface area changes: a.) Standard deviation of area variation versus mean surface area as a % of maximum, b.) Maximum lake size versus mean area as a % of maximum, and c.) Lake E/I versus area standard deviation of area variation. Red symbols indicate lakes sourced by snow and/or permafrost thaw.

Figure A2. Isotope data from the sub-set of lakes sampled during different seasons from Table A1. The arrow colors correspond to lake symbols and indicate the direction and magnitude of isotopic change for each lake.

Figure A3. Isotope data for the 175 lakes from Table A2, including the 54 lakes used for comparisons with lake area trends, shown by individual sampling campaigns carried out between Aug-Sept 2007 and July 2011. Top panel shows all data and lower panels show data for each campaign.

Figure A4. The distribution of δ^{18}O-intercept values on the GMWL from individual lake water δ^{18}O and δ^{2}H values regressed by an LEL with a slope of 5.

Figure A5: Lake isotope ratios shown with the Global Meteoric Water Line (GMWL), and estimated monthly precipitation values (black) [*Bowen and Wilkinson*, 2003], and Yukon, Porcupine and Chandalar River values (gray) [*Schuster et al.*, 2010]. Dashed arcs indicate the approximate ranges of isotope values for rain, snow, rivers, groundwater, and permafrost. Colors show the isotope ratios of lakes sampled within the five 11.2 km^2 plot areas (C, D, L, M, H) during July 2011 from *Heglund and Jones* [2003]. Plot locations are shown with the Yukon Flats National Wildlife boundary.